applied sciences

MDPI

Article

Virtual Antenna Arrays with Frequency Diversity for Radar Systems in Fifth-Generation Flying Ad Hoc Networks

Alberto Reyna [1,*], Jesús C. Garza [1], Luz I. Balderas [1], Jonathan Méndez [1], Marco A. Panduro [2], Gonzalo Maldonado [2] and Lourdes Y. García [1]

[1] Electronics Department, Autonomous University of Tamaulipas, Unidad Académica Multidisciplinaria Reynosa Rodhe (UAMRR), Carretera San Fernando cruce con Canal Rodhe, Reynosa 88779, Tamaulipas, Mexico; jesus.garza@uat.edu.mx (J.C.G.); luz.balderas@uat.edu.mx (L.I.B.); a2203728004@alumnos.uat.edu.mx (J.M.)

[2] CICESE Research Center, Electronics and Telecommunications Department, Carretera Ensenada-Tijuana No. 3918, Zona Playitas, Ensenada 22860, Baja California, Mexico

* Correspondence: alberto.reyna@docentes.uat.edu.mx

Abstract: This paper proposes the design of virtual antenna arrays with frequency diversity for radar systems in fifth-generation flying ad hoc networks. These virtual arrays permit us to detect targets from the sky with flying drones. Each array element is composed of a microstrip antenna mounted on quadcopter drones and is virtually connected with the other elements. The antennas are tuned to work at the lower fifth-generation frequency band of 3.5 GHz. The design process considers the optimization of frequency offsets and positions for each element to obtain a side lobe level reduction. This methodology is carried out by particle swarm optimization. Several design examples are presented with random frequency offsets and non-uniform positions. These designs are compared to uniform-spaced arrays excited with Hamming frequency offsets. The simulation results show that using random frequency offsets and non-uniform positions provides a minor side lobe level reduction. This research demonstrates the feasibility of using virtual arrays for radar systems in fifth-generation flying ad hoc networks.

Keywords: FANET; virtual antenna array; 5G; radar system; frequency diversity

Citation: Reyna, A.; Garza, J.C.; Balderas, L.I.; Méndez, J.; Panduro, M.A.; Maldonado, G.; García, L.Y. Virtual Antenna Arrays with Frequency Diversity for Radar Systems in Fifth-Generation Flying Ad Hoc Networks. *Appl. Sci.* **2024**, *14*, 4219. https://doi.org/10.3390/app14104219

Academic Editor: Atsushi Mase

Received: 15 April 2024
Revised: 3 May 2024
Accepted: 7 May 2024
Published: 16 May 2024

1. Introduction

Flying ad hoc networks (FANETs) facilitate many activities in society, such as agricultural processes, security, communications, and so on. This is possible with a swarm of drones wirelessly connected with low-gain antennas. In these swarms, the antenna system is crucial for effective performance; thanks to the antenna, it is possible to collect data from the sky with drones. However, reaching far targets is impossible when low-gain antennas are used. In recent years, the concept of virtual antenna arrays (VAAs), comprising a group of nodes formed by the low-gain antennas of each drone of the swarm [1–4], was introduced. This permits the antenna system to increase the directivity to reach far targets. Some interesting studies are being published on this topic; for instance, a polyhedral VAA with isotropic sources was studied with a direction-of-arrival estimation scheme [5]. In addition, the positions of isotropic sources were optimized to obtain high directivity and side lobe level reduction [6–8]. In [9], a comparison was made of a single element and a virtual linear array with the optimum service time when both used the same power. A non-uniform virtual array of isotropic sources was designed for an optimum side lobe, transmission power, and motion energy consumption [10]. A demonstration of the feasibility of VAA for multi-port input and multi-port output radars was reported in [11,12]. Previous research [13] proposed a sizeable VAA using a GPS to communicate over long distances. Research on forming a VAA to maintain an air object was reported in [14]. Other important papers have published VAAs based on the drone cluster approach in the presence

of position errors [15,16]. Recently, the effects of the drone structure in virtual arrays were studied in [8]. In addition, new research presented time-modulated VAAs with dipoles [17] and patch elements [18,19]. In summary, the previous works mainly proposed VAAs for communication systems of FANETs. However, the topic of VAAs is still maturing and has many opportune areas for research. In that context, this paper presents the application of VAAs for radar systems mounted on a FANET at 3.5 GHz. This frequency is very suitable for emerging radar systems in the fifth generation (5G). Previously, this scenario has not been studied in the literature. New FANETs will require communication with new 5G systems soon at the band of 3.5 GHz. To that end, we propose the design of frequency diversity virtual arrays (FDVAs) to detect objects in far targets with a 5G-FANET. It is important to highlight that frequency diversity has been utilized in traditional arrays [20], but not with virtual arrays. For instance, different frequency diversity arrays (FDAs) with a uniform linear topology were designed by using Hamming [21–23], logarithmic [24–28], and random frequency offsets [29–31]. These approaches generally utilize the spacing among the antennas of $\lambda/2$. On the other hand, two-dimensional topologies of FDAs, such as concentric rings [32] and rectangular [33], have been studied. In addition, three-dimensional spherical topologies were proposed in [34]. A novel FDA was also synthesized with time modulation [35]. These previous papers analyzed FDAs with isotropic antennas. Moreover, one piece of research [33] proposed an FDA with Yagi patch antennas. Here, the main contribution is the design of a non-uniform FDVA with elliptic patch antennas mounted on quadcopter drones. The main challenge was to find the optimum frequency offsets and positions of the nodes. This was achieved to obtain a side lobe level reduction. The methodology was carried out by particle swarm optimization (PSO). Several design examples with different numbers of antennas are presented.

2. Virtual Array Model

Each element of the FDVA consists of an elliptic patch antenna assembled on a quadcopter drone, as shown in Figure 1. The maximum size of the drone is 131 mm. The parts of the drone consist of metal and carbon fiber. The antenna is strategically located on the side of the drone to focus the radiation on the front.

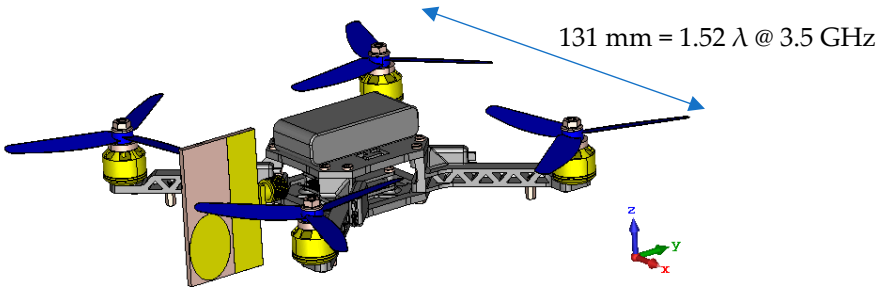

Figure 1. Element model of FDVA.

The radiation pattern for a VAA of N elements is formulated by the next formula [21],

$$P(\theta, d) = \sum_{n=1}^{N} g(\theta) e^{j(kx_n sin\theta + 2\pi(f_0+f_n)(d-d_0)/c)} \quad (1)$$

where θ is the elevation angle, and the wave number is defined as $k = 2\pi/\lambda$ with λ as the wavelength in the initial frequency f_0. The variable x_n is the element position in space. The term f_n is the frequency offset concerning f_0. The difference between frequency offsets is $\Delta f_n = (f_n - f_{n-1})$. The variable d is the distance variable. The term d_0 is the distance between the array and the maximum radiation. The constant c is the velocity of light in a vacuum. The function $g(\theta)$ is the element pattern of the nth antenna in the frequency f_0. This function considers the pattern distortion due to the aircraft structure depicted in Figure 1. The elliptical patch antenna is shown in Figure 2. The antenna material is an FR4

substrate of 1.6 mm thickness, with a permittivity of εr = 4.3, a tangential loss of δ = 0.0025, and a copper layer of 0.04 mm. The physical dimensions are W = 37.5 mm, L = 25 mm, G = 37.5 mm, R = 9 mm, r = 6.5 mm, h = 17.6 mm, x = 1.9 mm, and lg = 9 mm. The antenna parameters were calculated based on the theory reported in [36]. It should be noted that the radiation pattern of the FDVA was simulated in the CST microwave studio. The reflection coefficient is shown in Figure 3; this antenna operates from 3.25 GHz to 3.79 GHz. We selected this element because it is low profile, which is an important characteristic when the antenna is mounted on a drone. Nevertheless, the drone can use a different antenna element. The selection of the best antenna for a frequency diversity virtual array is an open research topic.

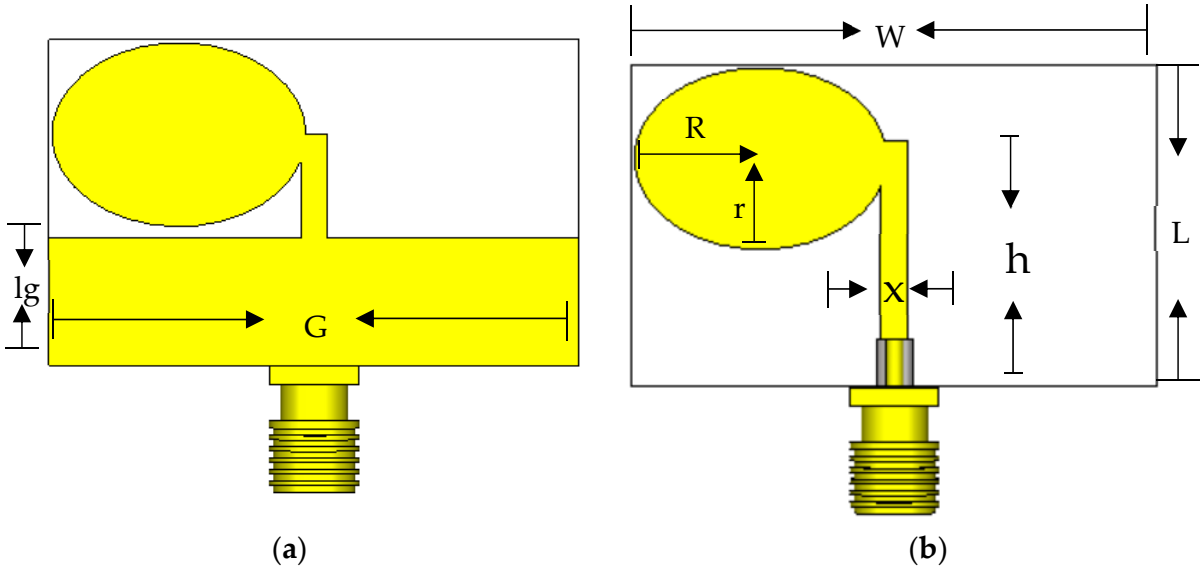

Figure 2. Antenna element: (**a**) back view; (**b**) front view.

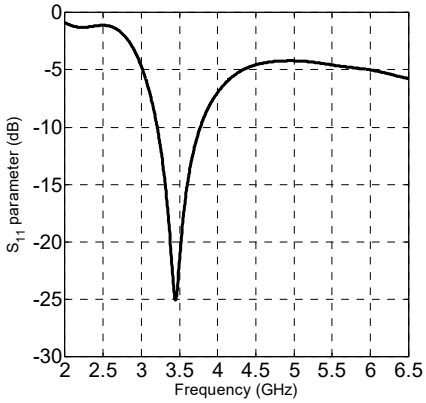

Figure 3. S_{11} parameter of the antenna element.

3. Problem Statement and Fitness Function

The design problem is to discover the optimum location coordinate x_n and frequency offset f_n for each element of the FDVA, to obtain optimum radiation patterns. The terms f_0 and d_0 are considered constants during the optimization process. In this scenario, the optimization variables are computed as,

$$Q = \left[q^1, q^2, \ldots, q^i\right] \tag{2}$$

$$q^i = \left[x_n^i, f_n^i\right] \tag{3}$$

The Q term is a matrix of optimization variables, and each element q^i represents the location x_n and the frequency offset f_n. The index term i is an individual from the swarm. During the optimization method, the spacings x_n are searched by defining a spacing $s_n = x_n - x_{n-1}$ among the drones within the range of $s_n \in [1.7\ \lambda, 2.7\ \lambda]$, where the wavelength λ is considering the frequency f_0 = 3.5 GHz. This constraint is to avoid a possible collision of drones. The frequency offsets, such as $f_n \in$ [1 KHz, 20 KHz], are also constrained. The objective function of this optimization is computed with the next expression:

$$of = \max(SLL) \tag{4}$$

SLL is the maximum side lobe level for the radiation patterns $P(\theta,d)$. The algorithm PSO minimizes the objective function *of*, obtaining the optimum radiation patterns defined in Equation (1). The methodology of PSO is taken as in [37]. This methodology is very efficient for the design of antenna arrays, as mentioned in [37]. However, we do not claim that PSO is the best algorithm for an FDVA. The design process used the PSO just as a tool to find the optimization variables. The next section will describe the simulation results.

4. Simulation Results

The particle swarm algorithm was coded in MATLAB under a computer with four Xeon processors (model E5-2640) and 256 GB of memory (RAM). The configuration of the PSO was set as follows: number of iterations i_{max} = 1800, number of agents p_{size} = 50, inertial weight w varies downward in the range of [0.95–0.4], and acceleration constants $c_1 = c_2 = 2$. This configuration has been tested with good results in antenna array optimization [37]. We established the FDVA with N = 6, 9, and 12 antenna elements. We performed cases with symmetry and no symmetry of the locations and frequency offsets around the origin. We summarize the results of the optimization in Table 1, which contains numerical values of the optimization variables x_n and f_n. In addition, Table 1 shows the values of the side lobe levels in a normalized magnitude. The cases with symmetry obtained better SLL reductions than those with no symmetry. Figure 4 shows the fitness function values during the optimization process for the cases with no symmetry. The PSO converges at the optimum solution. Figure 5 depicts the optimization variables' distributions. Using symmetrical distributions would decrease the hardware complexity of the antenna array. The symmetrical random distributions are better than the traditional Hamming distributions regarding SLL reductions.

Table 1. Optimization variables and fitness function values.

N	Symmetry	Normalized SLL	Directivity	Locations x_n (λ)	Frequencies f_n (KHz)
6	Yes	0.7706	6.56 dB	0, 1.7652, 4.4652, 7.0634, 9.7634, 11.5286	16.248, 12.135, 2.388, 2.388, 12.135, 16.248
9	Yes	0.5828	8.49 dB	0, 2.6582, 5.3208, 7.1053, 8.8719, 10.6385, 12.4230, 15.0856, 17.7438	19.744, 15.234, 12.436, 1.624, 4.664, 1.624, 12.436, 15.234, 19.744
12	Yes	0.5192	9.05 dB	0, 2.6613, 5.1533, 7.4415, 9.1495, 10.8621, 13.5126, 15.2252, 16.9332, 19.2214, 21.7134, 24.3747	10.57043, 19.94567, 17.6699, 1, 1.32935, 9.02219, 39.02219, 1.3293, 1, 17.6699 19.94567, 10.57043
6	No	0.7121	6.95 dB	0, 2.6412, 4.5123, 6.3544, 8.1316, 9.8321	14.3043, 19.217, 1, 1.7049, 11.1150, 2.5609
9	No	0.5904	8.43 dB	0, 2.6994, 5.3944, 8.0934, 9.8727, 12.5459, 14.3622, 16.0889, 17.8965	4.466, 3.308, 19.106, 0.1304, 1, 11.775, 1.171, 07.367, 18.245
12	No	0.5386	9.19 dB	0, 2.6986, 4.3989, 7.0827, 9.1845, 11.2371, 13.7306, 15.7537, 17.4566 19.1796, 20.9382, 23.6236	3.697, 19.408, 3.252, 6.969, 20.000, 13.671, 1, 19.997, 6.018, 17.358, 19.680, 12.929

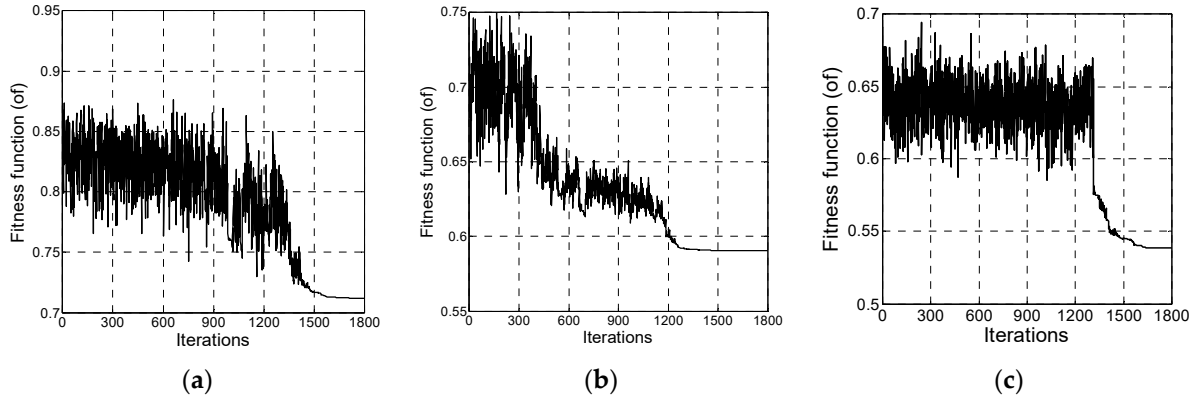

Figure 4. Fitness function during the optimization: (**a**) N = 6, (**b**) N = 9, and (**c**) N = 12.

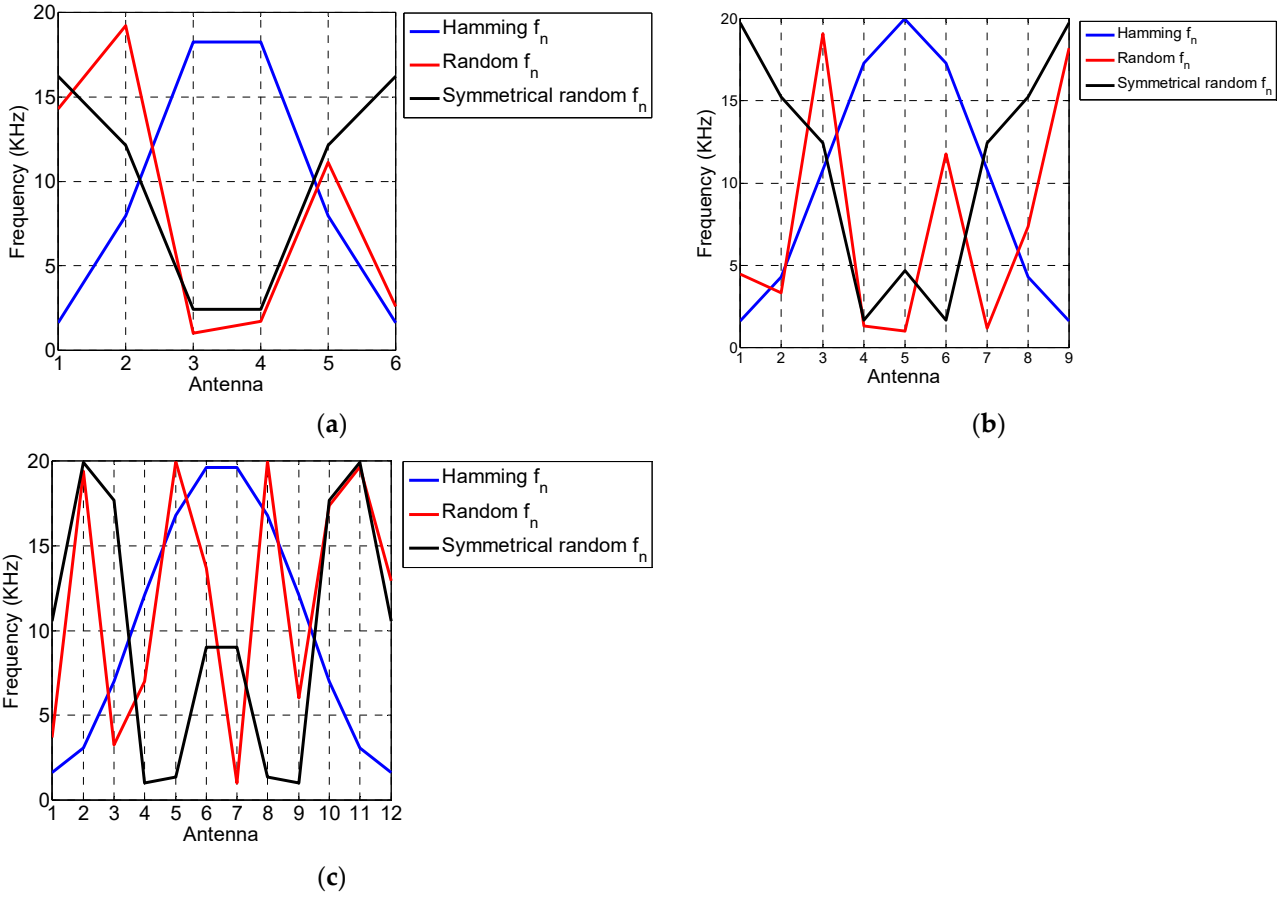

Figure 5. Optimization variable distributions: (**a**) N = 6, (**b**) N = 9, and (**c**) N = 12.

Now, these distributions generate the radiation patterns shown in Figures 6–8 for the cases with different numbers of antennas. Firstly, observe the radiation generated by the Hamming distribution in the three figures. These patterns contain grating lobes due to the spacing of the antennas at greater than $\lambda/2$. Nevertheless, it is impossible to use $\lambda/2$ as the spacing because this collides with the drones. In this case, the Hamming distributions are not suitable for this application. The random distributions obtain radiation with no grating lobes, as depicted in the three figures. One can infer that these distributions are better solutions for the FDVA. The symmetrical and non-symmetrical distributions generate similar patterns, and the SLL values change only slightly, although symmetrical distributions have the advantage of reducing hardware complexity.

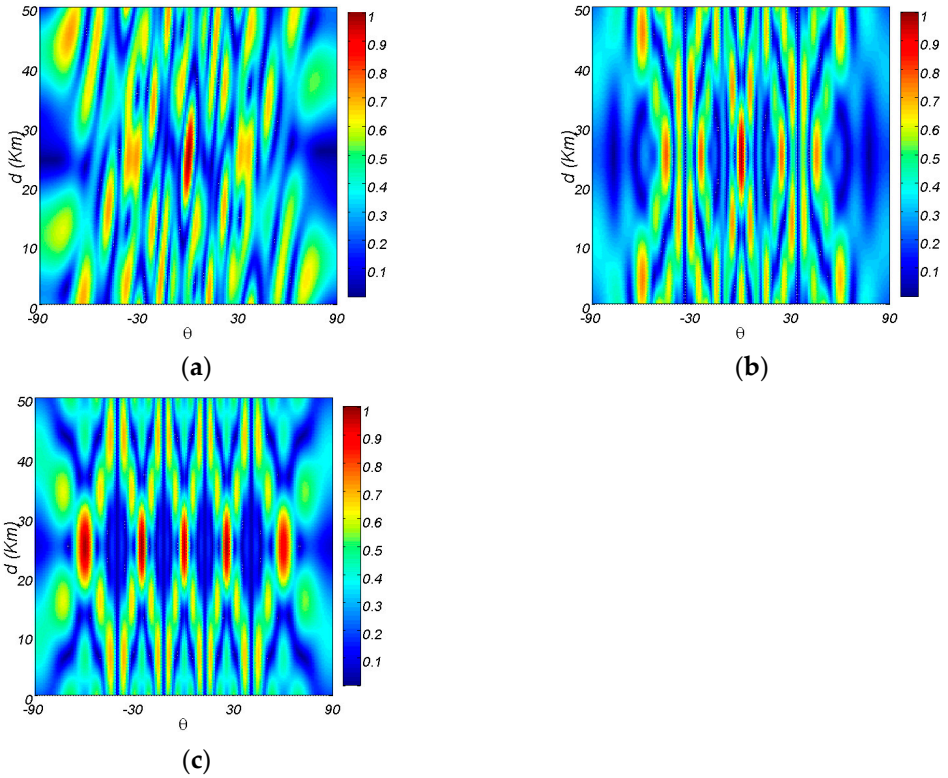

Figure 6. Radiation of a VAA with N = 6: (**a**) random without symmetry, (**b**) random with symmetry, and (**c**) Hamming S_{11} parameter of the antenna element.

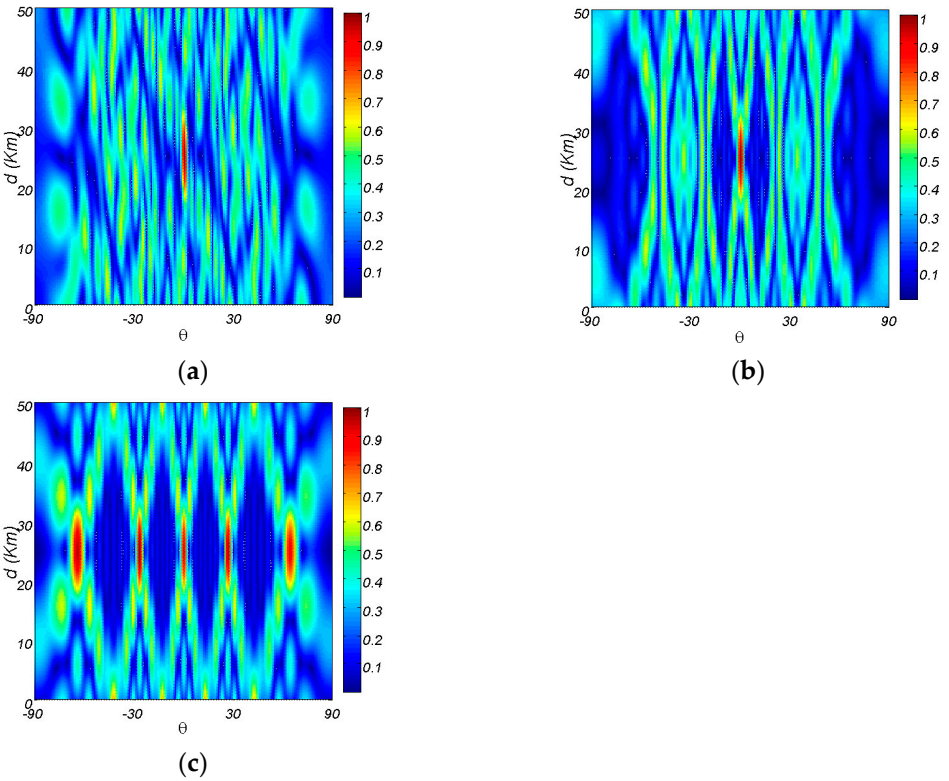

Figure 7. Radiation of a VAA with N = 9: (**a**) random without symmetry, (**b**) random with symmetry, and (**c**) Hamming distribution.

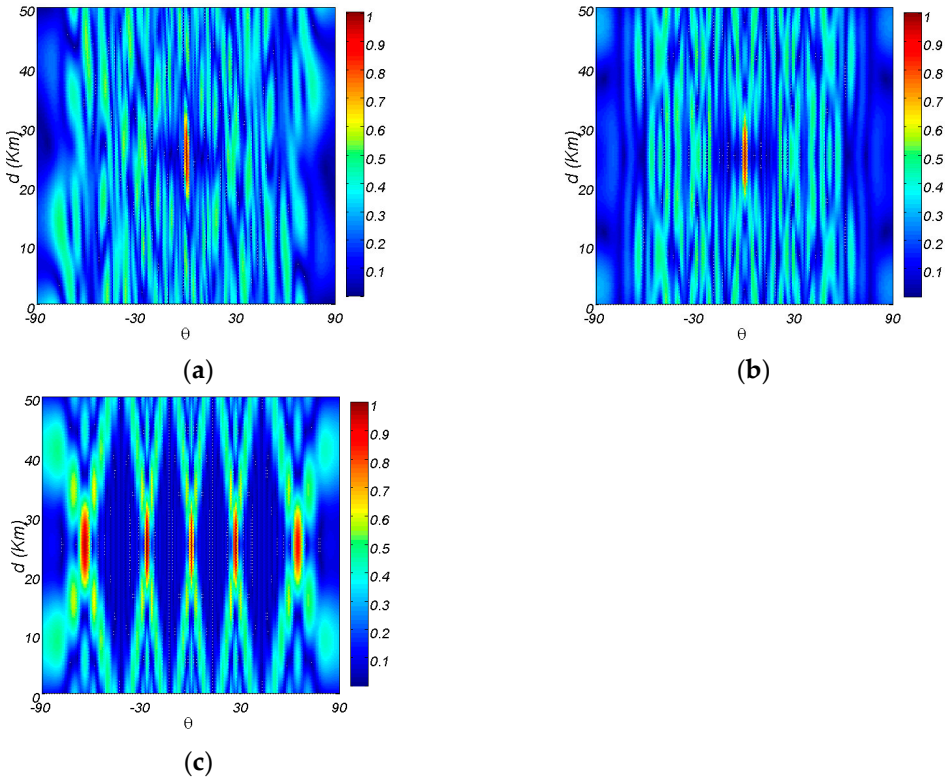

Figure 8. Radiation of a VAA with N = 12: (**a**) random without symmetry, (**b**) random with symmetry, and (**c**) Hamming distribution.

Table 2 contains a comparison with previous studies in the field of virtual antenna arrays. The main contribution of this work is the use of frequency diversity in virtual antenna arrays for 5G-FANETs. Moreover, most previous works used isotropic and dipole antennas with no drone structures. However, exploring the scenario of real antennas mounted on a drone is very important before real experimentation. Furthermore, other works utilized patch antennas at a frequency of 2.4 GHz. Here, the designs utilized the recently opened band of 3.5 GHz. Additionally, the previous papers designed virtual arrays with other techniques such as time modulation or only random positions. Previously, frequency diversity was not used in virtual arrays. As such, our contribution represents an advance in this topic, which permits the topic to mature. The frequency diversity in virtual antenna arrays may permit using a FANET as a radar system in future emerging applications.

Table 2. Comparison with virtual arrays.

Work	Array Topology	Type of Antenna	Frequency	Drone	Algorithm	Perturbations
Ref. [5]	3D polyhedral and linear	Isotropic	Not included	Not included	DOA	Not included
Ref. [6]	3D random	Isotropic	Not included	Not included	DEMO	Not included
Ref. [7]	3D random in 4 layers	Isotropic	Not included	Not included	Not included	Not included
Ref. [17]	Uniform linear and square with time modulation	Dipole	Not included	Not included	PSO	Not included
Ref. [9]	Non-uniform linear	Isotropic	Not included	Not included	Deterministic	Not included
Ref. [10]	3D random	Isotropic	Not included	Not included	DPINSGA-II	Not included

Table 2. *Cont.*

Work	Array Topology	Type of Antenna	Frequency	Drone	Algorithm	Perturbations
Ref. [15]	Non-uniform linear	Isotropic	Not included	Not included	Nelder mead simplex method	Included
Ref. [16]	Non-uniform linear	Isotropic	Not included	Not included	SOCP	Included
Ref. [8]	3D random	Square patch	2.4 GHz	Included	DEMO	Not included
Ref. [18]	Non-uniform linear with time modulation	Square patch	2.4 GHz	Not included	IWO	Not included
Ref. [19]	Non-uniform linear with time modulation	Fed-slot	2.4 GHz and 5.5 GHz	Included	DEMO	Included
This Work	Non-uniform linear with frequency diversity	Elliptic patch	3.25 GHz to 3.79 GHz	Included	PSO	Not Included

Finally, it is important to compare this study with previous papers in the field of FDAs. In this case, Table 3 compares the most representative works in this field. Most of these works present FDAs with linear topologies and isotropic antennas. The frequency offsets are Hamming, logarithmic, and random distributions. The main difference concerning this work is the combination of random frequency offsets and non-uniform antenna locations, the 5G frequency band, and the use of elliptic patch antennas mounted on real drones.

Table 3. Comparison with previous FDAs.

Work	Array Topology	Antenna	Frequency Offsets f_n	Initial Frequency f_0 and Uniform Δf_n	Distance d	Maximum Direction (d_0, θ_0)	Symmetry	Algorithm	Antenna Spacing
Ref. [24]	Linear N = 5, 10, 15, 17	Isotropic	Hamming and logarithmic	f_0 = 10 GHz Δf_n = 3 kHz, 2 kHz	0–2 km 2×10^5 km 0–90 km 0–1000 km	$\theta_0 = 0° \; 1 \times 10^5$ km 30° 500 km $\theta_0 = 0°$ 15 km, 45 km, 745 km $\theta_0 = 30°$ 500 km $\theta_0 = 0°$ 500 km	Yes/No	Not applied	λ λ/2 λ/4
Ref. [6]	Square N = 16, 8, 4	Patch Yagui 1–2 GHz 2–4 GHz	Not specified	Not specified	Not specified	$\theta_0 = 0°$	Not specified	Not applied	30 mm
Ref. [38]	Linear N = 10	Isotropic	Not specified	f_0 = 10 GHz Δf_n = 10 kHz	5–15 km	$\theta_0 = 0°$ 20 km	No	(CMT) algorithm	λ/2
Ref. [29]	Linear N = 10	Isotropic	Random	f_0 = 10 GHz Δf_n = 5 KHz.	0–25 km	$\theta_0 = 0° \; 0°$ $\theta_0 = 0° \; 1.91°$ 1 km $\theta_0 = 0° \; 56.44°$ 25 km	No	Not applied	λ/2
Ref. [25]	Linear N = 15	Isotropic	Logarithmic	f_0 = 5 GHz δ = 30 KHz $\Delta f_n = \log(m + 1)\delta$	0–60 km	$\theta_0 = 10°$ 25 km	Not specified	Not specified	λ/4
Ref. [26]	Linear N = 33	Isotropic	Hamming and logarithmic	f_0 = 10 GHz Δf_n = 85 kHz.	0–50 km	$\theta_0 = 0°$ 25 km	Yes	Not specified	0.24 m
Ref. [30]	Linear N = 16	Isotropic	Random	f_0 = 10 GHz $\Delta f_n \in$ [100 KHz–10,000 KHz]	10–15 km	$\theta_0 = \pi/3$ 10.11 km	No	Simulated annealing algorithm	Ref. [26]

Table 3. *Cont.*

Work	Array Topology	Antenna	Frequency Offsets f_n	Initial Frequency f_0 and Uniform Δf_n	Distance d	Maximum Direction (d_0, θ_0)	Symmetry	Algorithm	Antenna Spacing
Ref. [27]	Linear N = 10	Aperture antennas	Logarithmic and Hamming	f_0 = 10 GHz Δf_n = 50 KHz.	20–80 km	θ_0 = 20° 50 km	Yes	Genetic algorithm	0.015 m
Ref. [21]	Linear N = 20	Isotropic	Hamming	f_0 = 10 GHz	300–600 km	θ_0 = 0° 450 km	No	PSO	$\lambda/2$ = 0.015 m
Ref. [28]	Linear N = 16	Isotropic	Logarithmic	f_0 = 10 GHz, Δf_n = 30 KHz	50–100 km	θ_0 = 25° 75 km θ_0 = 0° 30° 82 km	No	Genetic algorithm, MUSIC algorithm	
Ref. [34]	Spherical random N = 18 elements	Isotropic	Not specified	Not specified	10–1000 km	θ_0 = 90° 100 km	No	Not specified	Not specified
Ref. [31]	Linear- rid N = 51	Isotropic	Random	f_0= 37.5 GHz carrier Δf_n = 1 MHz	Not specified	Not specified	No	BP-based 3D imaging algorithm	4 m
Ref. [39]	Linear N = 7 and 35	Isotropic	Not specified	f_0 = 10 GHz Δf_n = 4 KHz	15–45 km	θ_0 = 20° 30 km θ_0 = 0° 30 km	No	PSO algorithm	$\lambda/2$
Ref. [40]	Linear N = 23, 101	Isotropic	Not specified	f_0 = 3 GHz Δf_n = Not specified	0–20 km	θ_0 = 0° 10 km	No	Artificial bee colony (ABC) optimizer	$\lambda/2$
Ref. [23]	Linear N = 8	Isotropic	Hamming	f_0 = 10 GHz Δf_n = 10 KHz	15–45 km	θ_0 = 0° 30 km	No	PSO Algorithm	$\lambda/2$
Ref. [22]	Linear N = 5	Isotropic	Hamming	f_0 = 1 *GHz* Δf_n = 1 kHz, 10 MHz, 200 MHz	0–100 km	θ_0 = 0° 60 km	No	CLEAN algorithm	$\lambda/2$
This work	Non-uniform linear N= 6, 9 and 12	Elliptic patch	Random	f_0 = 3.5 GHz	0–50 km	θ_0 = 0° 25 km	Yes	PSO	Non-uniform

5. Conclusions

This paper has presented virtual antenna arrays with frequency diversity in the context of 5G communications at 3.5 GHz. We studied the performance of virtual arrays with random frequency offsets and non-uniform locations of the nodes. This combination of variables obtained better results in the radiation patterns than the traditional schemes of Hamming distributions with uniform antenna locations. The results demonstrate that these arrays can form a radar system with a FANET to detect objects from the sky. Future works will focus on validating the findings of this study with experimental tests.

Author Contributions: Conceptualization, A.R. and J.M.; methodology, A.R., J.C.G. and L.I.B.; software, A.R., J.M. and J.C.G.; validation, A.R., L.I.B. and M.A.P.; formal analysis, J.C.G. and A.R.; investigation, J.C.G., J.M. and L.I.B.; resources, A.R. and L.I.B.; data curation, J.C.G. and A.R.; writing—original draft preparation, G.M. and A.R.; writing—review and editing, J.M. and L.Y.G.; visualization, A.R. and M.A.P.; supervision, A.R.; project administration, A.R.; funding acquisition, A.R. and M.A.P. All authors have read and agreed to the published version of the manuscript.

Funding: The research work presented in this paper was supported by UAT with the project number UAT/SIP/INV/2023/060.

Institutional Review Board Statement: Not applicable.

Informed Consent Statement: Not applicable.

Data Availability Statement: The original contributions presented in the study are included in the article, further inquiries can be directed to the corresponding author.

Conflicts of Interest: The authors declare no conflicts of interest.

References

1. Dohler, M.; Aghvami, A.H. Distributed antennas: The concept of virtual antenna arrays. In *Cooperation in Wireless Networks: Principles and Applications*; Springer: Dordrecht, The Netherlands, 2006; pp. 421–461.
2. Lin, Z.; Lin, M.; de Cola, T.; Wang, J.-B.; Zhu, W.-P.; Cheng, J. Supporting IoT With Rate-Splitting Multiple Access in Satellite and Aerial-Integrated Networks. *IEEE Internet Things J.* **2021**, *8*, 11123–11134. [CrossRef]
3. Lin, Z.; Niu, H.; An, K.; Wang, Y.; Zheng, G.; Chatzinotas, S.; Hu, Y. Refracting RIS-Aided Hybrid Satellite-Terrestrial Relay Networks: Joint Beamforming Design and Optimization. *IEEE Trans. Aerosp. Electron. Syst.* **2022**, *58*, 3717–3724. [CrossRef]
4. Niu, H.; Chu, Z.; Zhou, F.; Zhu, Z.; Zhen, L.; Wong, K.-K. Robust Design for Intelligent Reflecting Surface-Assisted Secrecy SWIPT Network. *IEEE Trans. Wirel. Commun.* **2022**, *21*, 4133–4149. [CrossRef]
5. Keskin, F.; Filik, T. Isotropic and directional DOA estimation of the target by UAV swarm-based 3-D antenna array. In Proceedings of the 2020 4th International Symposium on Multidisciplinary Studies and Innovative Technologies (ISMSIT), Istanbul, Turkey, 22–24 October 2020; pp. 1–7.
6. Garza, J.; Panduro, M.A.; Reyna, A.; Romero, G.; Rio, C.D. Design of UAVs-based 3D antenna arrays for maximum performance in terms of directivity and SLL. *Int. J. Antennas Propag.* **2016**, *2016*, 2621862. [CrossRef]
7. Wang, W.; Zheng, Z.; Chen, M.; Zhang, H.; Liang, X. An unmanned aerial vehicle antenna array. In Proceedings of the 2020 IEEE International Symposium on Antennas and Propagation and North American Radio Science Meeting, Montréal, QC, Canada, 5–10 July 2020; pp. 183–184.
8. Reyna, A.; Garza, J.C.; Elizarrarás, O.; Panduro, M.; Balderas, L.I.; de la Luz Prado, M. 3D random virtual antenna arrays for FANETs wireless links. *Telecommun. Syst.* **2021**, *77*, 469–477. [CrossRef]
9. Mozaffari, M.; Saad, W.; Bennis, M.; Debbah, M. Drone-based antenna array for service time minimization in wireless networks. In Proceedings of the 2018 IEEE International Conference on Communications (ICC), Kansas, MO, USA, 20–24 May 2018; pp. 1–6.
10. Sun, G.; Zhao, X.; Shen, G.; Liu, Y.; Wang, A.; Jayaprakasam, S. Improving performance of distributed collaborative beamforming in mobile wireless sensor networks: A multi-objective optimization method. *IEEE Internet Things J.* **2020**, *7*, 6787–6801. [CrossRef]
11. Dohler, M.; Dominguez, J.; Aghvami, H. Link capacity analysis for virtual antenna arrays. In Proceedings of the IEEE 56th Vehicular Technology Conference, Vancouver, BC, Canada, 24–28 September 2002; Volume 1, pp. 440–443.
12. Wang, W.-Q. Virtual antenna array analysis for MIMO synthetic aperture radars. *Int. J. Antennas Propag.* **2012**, *2012*, 587276. [CrossRef]
13. Jan, S.S.; Enge, P. Using GPS to synthesize a large antenna aperture when the elements are mobile. In Proceedings of the 2000 National Technical Meeting of the Institute of Navigation, Anaheim, CA, USA, 26–28 January 2000; pp. 1–11.
14. Milyakov, D.A.; Verba, V.S.; Merkulov, V.I.; Plyashechnik, A.S. Quadcopter active phased antenna array. *Procedia Comput. Sci.* **2021**, *186*, 628–635. [CrossRef]
15. Breheny, S.H.; D'Andrea, R.; Miller, J.C. Using airborne vehicle-based antenna arrays to improve communications with UAV clusters. In Proceedings of the 42nd IEEE International Conference on Decision and Control, Maui, HI, USA, 9–12 December 2003; Volume 4, pp. 4158–4162.
16. Chandra, R.S.; Breheny, S.H.; D'Andrea, R. Antenna array synthesis with clusters of unmanned aerial vehicles. *Automatica* **2008**, *44*, 1976–1984. [CrossRef]
17. Reyna, A.; Panduro, M.A.; Mendez, A.; Balderas, L.; Del Río, C. Distributed antenna array for FANET's wireless links using time modulation. In Proceedings of the 2019 13th European Conference on Antennas and Propagation (EuCAP), Krakow, Poland, 31 March–5 April 2019; pp. 1–3.
18. Jiménez, D.A.; Reyna, A.; Panduro, M.A.; del Rio, C.; Ram, G.; Balderas, L. UAVs-based antenna arrays using time modulation. *Telecommun. Syst.* **2020**, *74*, 113–127. [CrossRef]
19. Garza, J.C.; Reyna, A.; Balderas, L.I.; Panduro, M.A.; García, L.Y. Dual-band virtual antenna array with time modulation in presence of position perturbations. *Telecommun. Syst.* **2022**, *81*, 539–547. [CrossRef]
20. Ma, R.; Yang, W.; Guan, X.; Lu, X.; Song, Y.; Chen, D. Covert mmWave Communications With Finite Blocklength Against Spatially Random Wardens. *IEEE Internet Things J.* **2024**, *11*, 3402–3416. [CrossRef]
21. Liao, Y.; Zeng, G.; Wu, C.; Wang, W.-Q.; Zheng, Z. Frequency Diverse Array Design for Deceptive Jamming Suppression Using Particle Swarm Optimization. In Proceedings of the 2021 IEEE International Geoscience and Remote Sensing Symposium IGARSS, Brussels, Belgium, 11–16 July 2021; pp. 2719–2722. [CrossRef]
22. Yong-Guang, C.; Yun-tao, L.; Yan-hong, W.; Hong, C. Research on the linear frequency diverse array performance. In Proceedings of the IEEE 10th International Conference on Signal Processing Proceedings, Beijing, China, 24–28 October 2010; pp. 2324–2327. [CrossRef]

23. Xu, Y.; Huang, X.; Wang, A. PSO-Based Low-SLL Pattern Synthesis for FDA in Range-Angle Space. In Proceedings of the 2022 International Conference on 6G Communications and IoT Technologies (6GIoTT), Fuzhou, China, 14–16 October 2022; pp. 20–24. [CrossRef]
24. Ahmad, Z.; Chen, M.; Bao, S.D. Beampattern analysis of frequency diverse array radar: A review. *J. Wirel. Commun. Netw.* **2021**, *2021*, 189. [CrossRef]
25. Zhang, L.; Xu, W.; Huang, P.; Tan, W. Comparison of Frequency Diverse Array Patterns with Nonuniform Frequency Offset. In Proceedings of the 2020 IEEE MTT-S International Wireless Symposium (IWS), Shanghai, China, 20–23 September 2020; pp. 1–3. [CrossRef]
26. Xu, W.; Zhang, L.; Bi, H.; Huang, P.; Tan, W. FDA Beampattern Synthesis With Both Nonuniform Frequency Offset and Array Spacing. *IEEE Antennas Wirel. Propag. Lett.* **2021**, *20*, 2354–2358. [CrossRef]
27. Shao, X.; Hu, T.; Xiao, Z.; Zhang, J. Frequency Diverse Array Beampattern Synthesis With Modified Sinusoidal Frequency Offset. *IEEE Antennas Wirel. Propag. Lett.* **2021**, *20*, 1784–1788. [CrossRef]
28. Xiong, J.; Wang, W.-Q.; Shao, H.; Chen, H. Frequency Diverse Array Transmit Beampattern Optimization With Genetic Algorithm. *IEEE Antennas Wirel. Propag. Lett.* **2017**, *16*, 469–472. [CrossRef]
29. Mai, C.; Lu, S.; Sun, J.; Wang, G. Beampattern Optimization for Frequency Diverse Array With Sparse Frequency Waveforms. *IEEE Access* **2017**, *5*, 17914–17926. [CrossRef]
30. Dai, M.; Wang, W.-Q.; Shao, H. FDA radar ambiguity function optimization with simulated annealing algorithm. In Proceedings of the 2015 Asia-Pacific Signal and Information Processing Association Annual Summit and Conference (APSIPA), Hong Kong, China, 16–19 December 2015; pp. 740–743. [CrossRef]
31. Shen, J.; Liao, K.; Ouyang, S.; Wang, H.; Yu, Q. Front-Downward-Looking 3D SAR Imaging Using Frequency Diversity Array. In Proceedings of the 2021 IEEE International Geoscience and Remote Sensing Symposium IGARSS, Brussels, Belgium, 11–16 July 2021; pp. 3967–3970. [CrossRef]
32. Akkoç, A.; Afacan, E.; Yazgan, E. Investigation of Planar Frequency Diverse Array Antenna in Concentric Circular Geometry. In Proceedings of the 2019 11th International Conference on Electrical and Electronics Engineering (ELECO), Bursa, Turkey, 28–30 November 2019; pp. 651–654. [CrossRef]
33. Sun, F.; Zhang, F.-S.; Zhang, H.; Zhang, H.; Li, C.; Feng, C. A Frequency Diversity Printed-Yagi Antenna Element for Apertures Selectivity Wideband Array Application. *IEEE Trans. Antennas Propag.* **2018**, *66*, 5634–5638. [CrossRef]
34. Adeyemi, T.; Buchanan, K. Frequency diverse scanning for aperiodic (Random) antenna arrays. In Proceedings of the 2016 IEEE International Symposium on Antennas and Propagation (APSURSI), Fajardo, PR, USA, 26 June–1 July 2016; pp. 923–924. [CrossRef]
35. Maneiro-Catoira, R.; Brégains, J.; García-Naya, J.A.; Castedo, L. A TMA-FDA Approach for Two-Beam Steering. *IEEE Antennas Wirel. Propag. Lett.* **2021**, *20*, 1973–1977. [CrossRef]
36. Ferdous, N.; Chin, G.; Hamid, S.H.A.; Nazri, M.; Raman, A.; Kiong, T.S.; Ismail, M. Design of a small patch antenna at 3.5 GHz for 5G application. IOP Conference Series: Earth and Environmental Science. In Proceedings of the International Conference on Sustainable Energy and Green Technology 2018, Kuala Lumpur, Malaysia, 11–14 December 2018. [CrossRef]
37. Panduro, M.A.; Brizuela, C.A.; Balderas, L.I.; Acosta, D.A. A Comparison of Genetic Algorithms, Particle Swarm Optimization and the Differential Evolution Method for the Design of Scannable Circular Antenna Arrays. *Prog. Electromagn. Res. B* **2009**, *13*, 171–186. [CrossRef]
38. Li, S.; Zong, Z.; Huang, L.; Feng, Y. Adaptive Null Optimization Method Based on Frequency Diverse Array. In Proceedings of the 2021 IEEE International Geoscience and Remote Sensing Symposium IGARSS, Brussels, Belgium, 12–16 July 2021; pp. 5012–5015. [CrossRef]
39. Xu, Y.; Shi, X.; Li, W.; Xu, J.; Huang, L. Low-Sidelobe Range-Angle Beamforming With FDA Using Multiple Parameter Optimization. *IEEE Trans. Aerosp. Electron. Syst.* **2019**, *55*, 2214–2225. [CrossRef]
40. Yang, Y.-Q.; Wang, H.; Wang, H.-Q.; Gu, S.-Q.; Xu, D.-L.; Quan, S.-L. Optimization of Sparse Frequency Diverse Array With Time-Invariant Spatial-Focusing Beampattern. *IEEE Antennas Wirel. Propag. Lett.* **2018**, *17*, 351–354. [CrossRef]